SCITECH
RESEARCH ORGANISATION|

Volume 16, Issue 3

Published online: July 04, 2020|

Journal of Progressive Research in Mathematics
www.scitecresearch.com/journals

Validating Numerical to Theoretical Solutions in a Reaction-Diffusion with Linear Cross-Diffusion Systems.

H . S. Ndakwo[1], Umar M. A[2], and Sulayman M. Bello[3]

Abstract

In this paper, we consider a reaction diffusion system with linear cross-diffusion. We carry out the analytical study in detail and find out that, when the diffusion coefficient is unity, Turing instability does not occur, but with the introduction of cross-diffusion, the system exhibit Turing instability. The numerical results reveal that, on increasing the value of, there is an occurrence of spatial patterns which conforms with the theoretical results. The cross-diffusion coefficients really play a vital role on the parameter spaces and spatial patterns of our system.

Keywords: Cross-diffusion driven instability, parameter space, spatial patterns, pattern formation, validation, numerical simulation, Turing theory, Finite difference method.

1 Introduction

The formation of patterns is one of the vital areas of research in mathematical biology. The popular one that mostly studied model for pattern formation is the reaction-diffusion which was proposed by Alan Turing in 1952 [37]. He demonstrated that a system of reacting and diffusing chemicals can evolve from initial near-homogeneity into a spatial pattern of chemical concentration. To describe the interaction between species in the areas of say, population dynamics, we usually investigate the general reaction-diffusion equations of the form

$\frac{\partial \boldsymbol{u}}{\partial t} = D\nabla \boldsymbol{u} + \boldsymbol{f}(\boldsymbol{u})$, where $D \in \mathbb{R}^{mxm}$ is a matrix of the diffusion coefficients and $\boldsymbol{f}$ is the reaction term. Here, we introduce cross-diffusion coefficient to the system.

In recent years, they have studied the Turing patterns similar to our model but have not really considered the negative diffusion, to see whether Turing patterns can occur outside the classical Turing parameter space. We study both positive and negative cross-diffusion, thereby selecting a point outside the classical parameter space to see whether there will be an emergence of spatial patterns, we then compare it with the theoretical analysis. Our work is organized as follows. In Section 2, we analyze our model, here we study under what conditions on the parameter values is the uniform steady state stable or unstable. We determine the parameter values that are outside the classical Turing diffusion-driven instability parameter space that are likely to give rise to pattern. In Section 3, this is where we derive the finite difference method that will be use for our numerical computations. In Section 4, we perform our numerical simulations by using finite difference method derived in Section 3 and the results are compare to the linear stability solutions, the whole process were implemented in MATLAB.

Finally, Section 5, is devoted to some discussions and conclusions.

*Corresponding author: hsndakwo@yahoo.com
[1]Department of Mathematics, Nasarawa State University, PMB 1022 Keffi. Nigeria
[2]Department of Mathematics, Nasarawa State University, PMB 1022 Keffi. Nigeria
[3]Department of Mathematics, Nasarawa State University, PMB 1022 Keffi. Nigeria

2 Model equations on stationary domains

Let $\Omega \subset \mathbb{R}^m$ $(m = 1, 2, 3)$ be a simply connected bounded stationary volume for all time $t \in I = [0, t_F]$, $t_F > 0$ and $\partial\Omega$ be the surface boundary enclosing Ω. Also let $\boldsymbol{u} = (u(\boldsymbol{x}, t), v(\boldsymbol{x}, t))^T$ be a vector of two chemical concentrations at position $\boldsymbol{x} = (x, y, z) \in \Omega \subset \mathbb{R}^m$. The evolution equations for reaction-diffusion systems with cross-diffusion can be obtained from the application of the law of mass conservation to yield the dimensional system.

$$\begin{cases} \begin{cases} u_t = D_u \nabla^2 u + D_{uv} \nabla^2 v + f_1(u, v), \\ v_t = D_v \nabla^2 v + D_{vu} \nabla^2 u + f_2(u, v), \end{cases} & x \in \Omega,\ t > 0, \\ \boldsymbol{n} \cdot \nabla u = \boldsymbol{n} \cdot \nabla v = 0,\ x \text{ on } \partial\Omega,\ t \geq 0, \\ u(x, 0) = u_0(x), \text{ and } v(x, 0) = v_0(x),\ x \text{ on } \Omega,\ t = 0, \end{cases} \tag{2.1}$$

where ∇^2 is the Laplace operator on domains and volumes, $D_u > 0$, $D_v > 0$, D_{uv} and D_{vu} are diffusion and cross-diffusion coefficients respectively. Here, $\boldsymbol{n}$ is the unit outward normal to $\partial\Omega$. Initial conditions are prescribed through non-negative bounded functions $u_0(x)$ and $v_0(x)$. In the above, $f_1(u, v)$ and $f_2(u, v)$ represent nonlinear reactions given by

$$f_1(u, v) = k_1 a_1 - k_2 u + k_3 u^2 v, \tag{2.2}$$

$$f_2(u, v) = k_4 b_1 - k_3 u^2 v, \tag{2.3}$$

where a_1, b_1, k_1, k_2, k_3 and k_4 are all positive constants.
For simplicity, we nondimensionalise equation (2.1) with the following scaling:

$$u = U^* \bar{u},\quad v = V^* \bar{v},\quad x = L\bar{x} \quad \text{and} \quad t = T\bar{t},$$

where $\bar{}$ denotes the non-dimensional variables. Substituting each of these variables into equation (2.1) with *activator-depleted* reaction kinetics (2.2) and (2.3) and without loss of generality, we drop the bars to obtain the following non-dimensional reaction-diffusion system with cross-diffusion of the general form

$$\begin{cases} \begin{cases} u_t &= \nabla^2 u + d_v \nabla^2 v + \gamma f(a - u + u^2 v), \\ v_t &= d\nabla^2 v + d_u \nabla^2 u + \gamma g(b - u^2 v), \end{cases} & x \in \Omega,\ t > 0, \\ \boldsymbol{n} \cdot \nabla u = \boldsymbol{n} \cdot \nabla v = 0,\ x \text{ on } \partial\Omega,\ t \geq 0, \\ u(x, 0) = u_0(x), \text{ and } v(x, 0) = v_0(x),\ x \text{ on } \Omega,\ t = 0, \end{cases} \tag{2.4}$$

where

$$d = \frac{D_v}{D_u} > 0,\ d_u = \frac{D_{vu}}{D_u},\ d_v = \frac{D_{uv}}{D_u},\ \gamma = \frac{L^2 k_2}{d_u},\ a = \frac{k_1 a_1 \sqrt{\frac{k_3}{k_2}}}{k_2} \text{ and } b = \frac{k_4 b_1 \sqrt{\frac{k_3}{k_2}}}{k_2}.$$

We note that d is the ratio of the diffusion coefficients only (without cross-diffusion), and d_u and d_v are the ratios of the cross-diffusion and the diffusion coefficients, respectively. In the next Subsection, we present a general linear stabilty analysis on cross-diffusion.

2.1 Linear stability analysis

In this Subsection, we would like to study under what conditions on the parameter values is the uniform steady state stable in the absence of diffusion and cross-diffusion and under what conditions it is unstable when diffusion and cross-diffusion are introduced, thereby giving rise to

the emergence of an inhomogeneous spatial structure [37, 32].
We proceed to investigate the possibility of cross-diffusion-driven by first expanding $\boldsymbol{u}(\boldsymbol{x},t)$ about the spatially independent uniform steady state solution $(u_s,v_s)^T$. Thus substituting

$$\begin{cases} u(\boldsymbol{x},t) = u_s + \eta w(\boldsymbol{x},t) \\ v(\boldsymbol{x},t) = u_s + \eta \psi(\boldsymbol{x},t) \end{cases} \quad \text{with } \eta \ll 1, \tag{2.5}$$

into system (2.4); on neglect of $O(\eta^2)$ and higher order terms, we obtain the following linearised reaction-diffusion system with cross-diffusion, written compactly in vector form

$$\boldsymbol{\Psi}_t = \gamma \boldsymbol{J_F} \boldsymbol{\Psi} + \boldsymbol{D}\nabla^2 \boldsymbol{\Psi}, \tag{2.6}$$

with

$$\boldsymbol{F} = \begin{pmatrix} f(u,v) \\ g(u,v) \end{pmatrix}, \ \boldsymbol{J_F} = \begin{pmatrix} \frac{\partial f}{\partial u} & \frac{\partial f}{\partial v} \\ \frac{\partial g}{\partial u} & \frac{\partial g}{\partial v} \end{pmatrix} \equiv \begin{pmatrix} f_u & f_v \\ g_u & g_v \end{pmatrix}\Big|_{(u_s,v_s)}, \ \boldsymbol{D} = \begin{pmatrix} 1 & d_v \\ d_u & d \end{pmatrix} \text{ and } \boldsymbol{\Psi} = \begin{pmatrix} \omega \\ \psi \end{pmatrix}, \tag{2.7}$$

where $\boldsymbol{F}$ denotes the vector with reaction kinetics, $\boldsymbol{J_F}$ denotes the Jacobian matrix evaluated at (u_s,v_s), $\boldsymbol{D}$ denotes a matrix whose entries are the ratios of the regular diffusion and cross-diffusion coefficients and $\boldsymbol{\Psi}$ denotes the vector of solutions to the linear system of partial differential equations, respectively. We can solve analytically the linear system (2.6) using separation of variables to obtain a power series solution of the general form

$$\boldsymbol{\Psi}(\boldsymbol{x},t) = \sum_k b_k e^{\lambda(k^2)t} \boldsymbol{\Phi}_k(\boldsymbol{x}), \tag{2.8}$$

where for each k, Φ_k is the eigenfunction of the Laplace operator solving the Helmholtz equation

$$\begin{cases} \nabla^2 \Phi_k + k^2 \Phi_k = 0 & \text{on } \Omega, \\ (\boldsymbol{n}\cdot\nabla)\Phi_k = 0 & \text{on } \partial\Omega, \end{cases} \tag{2.9}$$

where k is the wavenumber. For each k, we substitute each $b_k e^{\lambda(k^2)t}\Phi_k$ into (2.6) to obtain

$$\left(\lambda \boldsymbol{I} - \gamma \boldsymbol{J_F} + k^2 \boldsymbol{D}\right) \Phi_k b_k = \boldsymbol{0}, \tag{2.10}$$

where $\boldsymbol{I}$ is an identity matrix. Since we require non-zero solutions, b_k and Φ_k are non-zero and therefore the matrix multiplying these must be singular. This entails that

$$\left|\lambda \boldsymbol{I} - \gamma \boldsymbol{J_F} + k^2 \boldsymbol{D}\right| = \begin{vmatrix} \lambda - \gamma f_u + k^2 & -\gamma f_v + d_v k^2 \\ -\gamma g_u + d_u k^2 & \lambda - \gamma g_v + d k^2 \end{vmatrix} = 0. \tag{2.11}$$

Thus $\lambda(k^2)$ satisfies the dispersion relation

$$\lambda^2 + b(k^2)\,\lambda + c(k^2) = 0 \tag{2.12}$$

where

$$b(k^2) = k^2(1+d) - \gamma(f_u + g_v), \tag{2.13}$$
$$c(k^2) = (d - d_u d_v)k^4 - \gamma k^2(d f_u + g_v - d_u f_v - d_v g_u) + \gamma^2(f_u g_v - f_v g_u), \tag{2.14}$$

with u, v, $f(u,v)$, $g(u,v)$ the scalar variables and kinetic functions in equation (2.4). The partial derivatives are evaluated in terms of the uniform steady state (u_s,v_s). Solutions to the dispersion relation (2.12) are given by

$$2\lambda(k^2) = -b(k^2) \pm \sqrt{b^2(k^2) - 4c(k^2)}. \tag{2.15}$$

Taking $k = 0$ we have the absence of diffusion and cross-diffusion and thus spatial homogeneity. Requiring that for (u_s, v_s) to be stable to the $k = 0$, spatially homogeneous, mode entails

$$\mathrm{Re}[\lambda(0)] = \mathrm{Re}\Big[-b(0) \pm \sqrt{b^2(0) - 4c(0)} \Big] < 0. \tag{2.16}$$

This is guaranteed provided $b(0) > 0$ and $c(0) > 0$ if and only if the following conditions hold

$$\mathrm{Trace}(\boldsymbol{J_F}) := f_u + g_v < 0, \tag{2.17}$$
$$\mathrm{Det}(\boldsymbol{J_F}) := f_u\, g_v - f_v\, g_u > 0. \tag{2.18}$$

These two conditions are independent of the effects of cross-diffusion and hence are identical to the conditions in the absence of cross-diffusion. The next three conditions highlight the differences between classical diffusively-driven conditions in the absence of cross-diffusion to those when it is present. In the presence of diffusion and cross-diffusion ($k^2 > 0$), we have

$$b(k^2) = k^2(1 + d) + b(0) > 0 \tag{2.19}$$

since $b(0) > 0$. For (u_s, v_s) to become unstable, we require that

$$\mathrm{Re}[\lambda(k^2)] > 0 \quad \text{for some } k^2 \text{ non-zero}, \tag{2.20}$$

thereby requiring that $c(k^2) < 0$ for some k^2 non-zero. By definition of $c(k^2)$ we can further re-arrange to obtain a quadratic polynomial in k^2 of the form

$$c(k^2) = P_2 k^4 + P_1 k^2 + c(0) \tag{2.21}$$

where

$$\begin{aligned} P_2 &= d - d_u d_v := \mathrm{Det}(\boldsymbol{D}), \\ P_1 &= \gamma(d_u f_v + d_v g_u - (d f_u + g_v)), \\ c(0) &= \gamma^2(f_u g_v - f_v g_u) > 0. \end{aligned}$$

In order to have a upward opening parabola (i.e. $c(k^2) < 0$ for some non-zero $k > 0$), we require the following condition on the relationship between diffusion and cross-diffusion coefficients to hold:

$$\mathrm{Det}(\boldsymbol{D}) = d - d_u d_v > 0. \tag{2.22}$$

This is the first of the three conditions necessary for cross-diffusion induced driven-instability. Now, in order for $c(k^2) < 0$ for some k^2 non-zero, we require that $P_1 < 0$. Therefore, the second condition for diffusion-driven instability in presence of cross-diffusion is given by

$$d f_u + g_v - d_u f_v - d_v g_u > 0. \tag{2.23}$$

For diffusively-driven instability to occur, we also require that there exists real $k_\pm^2$ such that $c(k_\pm^2) = 0$ and these can be easily shown to be given by

$$k_\pm^2 = \frac{-P_1 \pm \sqrt{P_1^2 - 4c(0)(d - d_u d_v)}}{2(d - d_u dv)}. \tag{2.24}$$

Thus, requiring $c(k^2) < 0$ entails $P_1^2 - 4c(0)(d - d_u d_v) > 0$, thereby yielding the third and last condition for cross-diffusion-driven-instability

$$(d f_u + g_v - d_u f_v - d_v g_u)^2 - 4(d - d_u d_v)(f_u g_v - f_v g_u) > 0. \tag{2.25}$$

The last condition can be obtained equivalently by imposing the requirement that $c(k^2) < 0$ for some $k \neq 0$, which is equivalent to requiring that the minimum $c_{min} < 0$. Differentiating $c(k^2)$ with respect to k^2 and setting to zero yields

$$2(d - d_u d_v)k^2 - \gamma(d f_u + g_v - d_u f_v - d_v g_u) = 0. \tag{2.26}$$

Solving for k^2 we obtain

$$k^2 = \gamma \left(\frac{df_u + g_v - d_u f_v - d_v g_u}{2(d - d_u d_v)} \right). \tag{2.27}$$

Substituting the above equation into $c(k^2)$ we have

$$c_{min} = \gamma^2 \left[(f_u g_v - f_v g_u) - \frac{(df_u + g_v - d_u f_v - d_v g_u)^2}{4(d - d_v d_u)} \right]. \tag{2.28}$$

Thus, the condition that $c(k^2) < 0$ for some non-zero k^2 is given by

$$\frac{(df_u + g_v - d_u f_v - d_v g_u)^2}{4(d - d_v d_u)} > (f_u g_v - f_v g_u), \tag{2.29}$$

to yield (2.25). We are now in a position to state the following theorem whose proof is given above:

Theorem 2.1 (Conditions for cross-diffusion driven instability). *The necessary conditions for cross-diffusion driven instability are given by:*

$$f_u + g_v < 0, \tag{2.30}$$
$$f_u g_v - f_v g_u > 0, \tag{2.31}$$
$$d - d_u d_v > 0 \tag{2.32}$$
$$df_u + g_v - d_u f_v - d_v g_u > 0, \tag{2.33}$$
$$(df_u + g_v - d_u f_v - d_v g_u)^2 - 4\,(d - d_v d_u)\,(f_u g_v - f_v g_u) > 0. \tag{2.34}$$

In the above, the subscripts u, v denote partial differentiation, with the Jacobian components f_u, f_v, g_u and g_v evaluated in terms of (u_s, v_s). The conditions (2.30) - (2.34) define a parameter space, in which the uniform steady state (u_s, v_s) is linearly unstable.

Eigenfunctions in one dimension and two dimensions

We shall investigate typical solutions to equation (2.9), they solutions obtained will be used to check the validity and consistency of our numerical technique. In order to determine the value of k^2 in equation (2.9), we use the separation of variables to solve for an eigenfunction and a wavenumber such that the eigenvalue problem is satisfied. The solution to equation (2.9) on the one dimensional domain $[0, 1]$ is given by

$$\Phi_n(x) = \cos(n\pi x), \; n = 1, 2.... \tag{2.35}$$

The wavenumbers here have the form $k_n^2 = n^2\pi^2$. And the general solution is given by

$$\Psi(x, t) = \sum_n \mathbf{b_n} \exp[\lambda(n^2\pi^2)t] \cos(n\pi x). \tag{2.36}$$

We consider, for example the wavenumbers $k_1^2 = \pi^2$, $k_2^2 = 2^2\pi^2$, $k_3^2 = 3^2\pi^2$ and $k_4^2 = 4^2\pi^2$ with their corresponding eigenfunctions $\cos(\pi x)$, $\cos(2\pi x)$, $\cos(3\pi x)$ and $\cos(4\pi x)$ respectively. But in two dimension, it is not possible to write a simple form of the eigenfunctions, unless the geometry is simple.
We consider a square domain defined by

$$R = \{(x, y) \in \mathbb{R}^2 : 0 \le x \le 1, \; 0 \le y \le 1\}.$$

The eigenfunctions are of the form

$$\Phi_{m,n}(x, y) = \cos(m\pi x) \cos(n\pi y), \tag{2.37}$$

with wavenumbers

$$k_{m,n}^2 = \pi^2(m^2 + n^2),$$

where m and n are integers. The general solution in this case is given by

$$\Psi(x,y,t) = \sum_{m,n\in H} \boldsymbol{b_{m,n}} \exp[\lambda(k^2_{m,n})t]\cos(m\pi x)\cos(n\pi y). \tag{2.38}$$

In two dimension, we consider the wavenumbers $k^2_{1,0}$, $k^2_{2,0}$, $k^2_{3,0}$ and $k^2_{4,0}$ with their corresponding eigenfunctions $\cos(\pi x)$, $\cos(2\pi x)$,
$\cos(3\pi x)$ and $\cos(4\pi x)$ respectively. The plots are presented in Fig. 4 which we compare with the numerical solutions.

The next step is to determine the parameter values that will satisfy conditions ((2.30)-(2.34)).

2.1.1 Determination of parameter values

In order to compare the linear stability results with the numerical solutions, it is important to identify the parameter values, these parameter values must satisfy the inequalities (2.30)-(2.34). Therefore, we select these parameter values such that they belong to the cross-diffusion induced driven instability region and lie outside the classical Turing diffusion-driven instability parameter space. The theoretical details of how these spaces are obtained are given in [25]. To this end, we consider the following cases:

case 1

- *Reaction diffusion system in the presence of cross-diffusion in both u and v components (that is $d_v = 1$ and $d_u = 1$) (blue),*
- *Reaction diffusion system in the absence of cross-diffusion (that is $d_u = 0$ and $d_v = 0$) (green).*
  For illustrative purposes, we fix $d = 10$ and for each case, we plot the parameter spaces on the same diagram in order to show the emergence of cross-diffusion parameter spaces. Fig. 1, demonstrate the classical Turing diffusion-driven parameter spaces (shown in green) and those induced by cross-diffusion on both components (shown in blue). Our intension is to

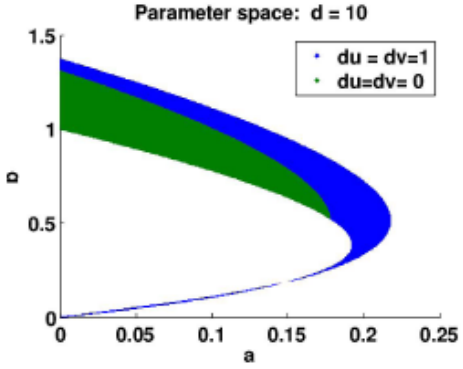

Figure 1: Plots demonstrating classical Turing parameter spaces with those induce by cross-diffusion. The green space is the classical Turing parameter region while the blue is the space induced by cross-diffusion.

compute patterns outside the classical Turing parameter space. Now, it is possible to select $a = 0.2$ and $b = 0.4$, a point outside the classical Turing parameter space (blue).

Case 2

- *We take $d = 1$*, and in the absence of cross-diffusion, the classical Turing diffusion driven-instability parameter space will not yield any patterns for all values of a and b (see Fig. 2

(d) to back-up this observation).
Next, we introduce cross-diffusion through the following cases:

- *The case when one of the cross-diffusion coefficient is absent that is* $d_u = 0$, *we take* $d_v = 0.8$ *and* $d = 1$ (see Fig. 2 (a)),
- *The case when one of the cross-diffusion coefficient is negative, that is negative cross-diffusion induced parameter spaces. Here, we take* $d_u = -0.8$, $d_v = 1$ *and* $d = 1$ (see Fig. 2 (b)) and
- *The case when* $d_u = 1$, $d_v = 0.8$ *and* $d = 1$ (see Fig. 2 (c)).

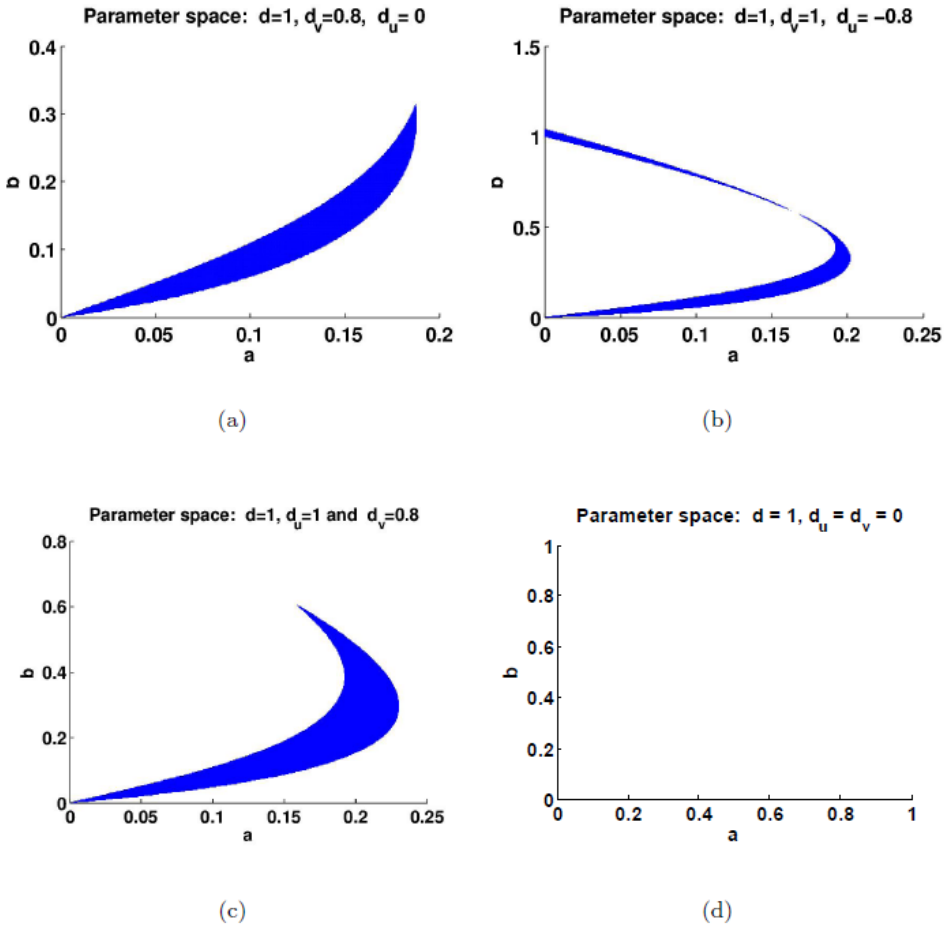

Figure 2: Plots demonstrating classical Turing parameter spaces with those induced by cross-diffusion, (a) when one of the cross-diffusion coefficient is absent i.e $d_u = 0$, $d_v = 0.8$ and $d = 1$, (b) when one of the cross-diffusion coefficient is negative i.e $d_u = -0.8$, $d_v = 1$ and $d = 1$, (c) $d_u = 1$, $d_v = 0.8$ and $d = 1$ and (d) when both cross-diffusion coefficients are absent with $d = 1$.

We are now in a position to select parameter values $a = 0.15$ and $b = 0.18$ from the space shown in Fig. 2 (a), $a = 0.15$ and $b = 0.2$ from the space shown in Fig. 2 (b), $a = 0.2$ and $b = 0.4$ from the space shown in Fig. 2 (c) to obtain cross-diffusion induced patterns in Figs. 4 and (d) no parameter value is selected since there is no parameter space seen.

The next step, we outline the finite difference method used to compute numerical simulations.

3 Finite difference method

Generally, numerical methods are use to compute the solutions of nonlinear or complicated ordinary differential equations. There are several numerical methods for solving differential equations, but here we use finite difference method to solve our system. Nowadays, numerical solutions are usually calculated on computers and the use of this method require an efficient use of programming languages and techniques. There are several of this languages presently in use, but in this research, we restrict ourself to Matlab because it is more suitable for graphing and is usually sufficient to illustrate the use of a numerical techniques.
We first consider the u-component of equation (2.4) of the form

$$u_t = \nabla^2 u + d_v \nabla^2 v + \gamma f(u, v). \tag{3.1}$$

We partition the domain in space using a mesh $x_0, x_1, ..., x_i$ and in time using a mesh $t_0, t_1, ..., t_N$, and we assume a uniform partition for both time and space.
We first discretize the Laplacian $\nabla^2 u$ for the case of one dimensional space $1D$ as follows: We let $u = u(x)$ so that, on expanding in Taylor series around a point $x = a$, we have

$$u(a + \Delta x) = u(a) + u'(a)\Delta x + \frac{1}{2}u''(a)\Delta x^2 + O(\Delta x^3), \tag{3.2}$$

$$u(a - \Delta x) = u(a) - u'(a)\Delta x + \frac{1}{2}u''(a)\Delta x^2 + O(\Delta x^3). \tag{3.3}$$

For the ease of our computer program, we hereby change our notation by replacing $u(a)$ by $u(i)$, $u(a + \Delta x)$ by $u(i + 1)$ similarly, $u(a - \Delta x)$ by $u(i - 1)$. By adding (3.2) and (3.3) and neglecting the terms with $O(\Delta x^3)$, we have

$$u''(i) = \frac{u(i + 1) - 2u(i) + u(i - 1)}{\Delta x^2}. \tag{3.4}$$

Similarly for v-component we have

$$v''(i) = \frac{v(i + 1) - 2v(i) + v(i - 1)}{\Delta x^2} \tag{3.5}$$

and the discretization of the time derivative is simply

$$u_t = \frac{u(i, j + 1) - u(i, j)}{\Delta t}. \tag{3.6}$$

By substituting equations (3.4) - (3.6) into (3.1) we have

$$u_{n+1} = u_n + \Delta t \gamma f(u, v) + \frac{\Delta t \left[u_1 + u_2 - 2u_0\right] + \Delta t d_v \left[v_1 + v_2 - 2v_0\right]}{h^2}, \tag{3.7}$$

where we denote $u(i, j + 1) = u_{n+1}, u(i, j) = u_n, u(i - 1) = u_1, u(i + 1) = u_2, u(i) = u_0, v(i - 1) = v_1, v(i + 1) = v_2, v(i) = v_0, \Delta x^2 = h^2$ which we refer to as the step size and Δt is the time step, these are all evaluated at the main time stepping loop.
Similarly, for the v-component we have

$$v_{n+1} = v_n + \Delta t \gamma g(u, v) + \frac{\Delta t d \left[v_1 + v_2 - 2v_0\right] + \Delta t d_u \left[u_1 + u_2 - 2u_0\right]}{h^2}. \tag{3.8}$$

Thus, we use equations (3.7)-(3.8) for our numerical computations in one dimensional space $(1D)$. The next step, we consider the case of two dimensional space, that is $\nabla^2 u = u_{xx} + u_{yy}$, we then discretize the Laplacian as follows: Here, we let $u = u(x, y)$, where (x, y) are two dimensional area which are divided up using a Cartesian grid and we use two indices to indicate where a quantity is being evaluated, this is similar to the case of one-dimensional space, the only difference is that, here we have two variables. Now we first consider the x-direction and then the y-direction as

follows:
In the x-direction, $\Delta x = x(i+1,j) - x(i,j) = x(i,j) - x(i-1,j)$ and
in the y-direction we have, $\Delta y = x(i,j+1) - x(i,j) = x(i,j) - x(i,j-1)$.
Using Taylor series around a point (i,j) yields

$$u(i+1,j) = u(i,j) + u_x(i,j)\Delta x + \frac{1}{2}u_{xx}(i,j)\Delta x^2 + O(\Delta x^3), \tag{3.9}$$

$$u(i-1,j) = u(i,j) - u_x(i,j)\Delta x + \frac{1}{2}u_{xx}(i,j)\Delta x^2 + O(\Delta x^3), \tag{3.10}$$

$$u(i,j+1) = u(i,j) + u_y(i,j)\Delta y + \frac{1}{2}u_{yy}(i,j)\Delta y^2 + O(\Delta y^3), \tag{3.11}$$

$$u(i,j-1) = u(i,j) - u_y(i,j)\Delta y + \frac{1}{2}u_{yy}(i,j)\Delta y^2 + O(\Delta y^3). \tag{3.12}$$

By adding equation (3.9) to (3.10) and (3.11) to (3.12) and neglecting the term with $O(\Delta x^3)$.., we have approximations to our derivatives as

$$u_{xx}(i,j) = \frac{u(i+1,j) + u(i-1,j) - 2u(i,j)}{\Delta x^2}, \tag{3.13}$$

$$u_{yy}(i,j) = \frac{u(i,j+1) + u(i,j-1) - 2u(i,j)}{\Delta y^2}. \tag{3.14}$$

Adding equation (3.13) to (3.14) gives

$$\nabla^2 u = \frac{u(i+1,j) + u(i-1,j) - 2u(i,j)}{\Delta x^2} + \frac{u(i,j+1) + u(i,j-1) - 2u(i,j)}{\Delta y^2}. \tag{3.15}$$

For convenience sake, we take $\Delta x = \Delta y = h$, this becomes

$$\nabla^2 u = \frac{u(i+1,j) + u(i-1,j) + u(i,j+1) + u(i,j-1) - 4u(i,j)}{h^2}. \tag{3.16}$$

Similarly for the v-component we have

$$\nabla^2 v = \frac{v(i+1,j) + v(i-1,j) + v(i,j+1) + v(i,j-1) - 4v(i,j)}{h^2}. \tag{3.17}$$

Substituting (3.16) and (3.17) into (3.1) just the same way we did for one-dimensional case we have

$$u_{n+1} = u_n + \Delta t\gamma f(u,v) + \frac{\Delta t\left[u_1 + u_2 + u_3 + u_4 - 4u_n\right] + \Delta t d_v\left[v_1 + v_2 + v_3 + v_4 - 4v_n\right]}{h^2}. \tag{3.18}$$

And for the v-component we follow the same procedure above, this gives

$$v_{n+1} = v_n + \Delta t\gamma g(u,v) + \frac{\Delta t d\left[v_1 + v_2 + v_3 + v_4 - 4v_n\right] + \Delta t d_u\left[u_1 + u_2 + u_3 + u_4 - 4u_n\right]}{h^2}. \tag{3.19}$$

where we denote $u(i,j+1) = u_{n+1}, u(i,j) = u_n, u(i-1,j) = u_1, u(i+1,j) = u_2, u(i,j-1) = u_3, u(i,j+1) = u_4, v(i,j) = v_n, v(i-1,j) = v_1, v(i+1,j) = v_2, v(i,j-1) = v_3, v(i,j+1) = v_4$, h and Δt are step-size and time-step respectively.
Thus, we use equations (3.18)-(3.19) for our numerical computations in two dimensional space $(2D)$.

4 Numerical solutions

In this Section, we compute numerical simulations of the spatial model (2.4) in both one and two space dimensions, and the qualitative results are shown here.

4.1 Numerical solution in 1D

We perform extensively numerical solution in one-dimensional space. All our numerical simulations emply the zero-flux boundary conditions, the number (N) of points is 100, with a space stepsize $h = \frac{1}{100}$ and a small time stepsize $\Delta t = h^3$. Other parameters are set as in Table 1. The numerical solution here, is computed using the finite difference method. All numerical tests were carried out by means of MATLAB. Fig. 3 (left and right) are solutions predicted by linear stability theory and numerical solutions respectively.

Figure	a	b	d	d_u	d_v	γ	initial condition
Figs.(3 and 4) (b)	0.2	0.4	1	1	0.8	8	$0.6 + 0.1 * cos(x)$
Figs.(3 and 4) (d)	0.2	0.4	1	1	0.8	20	$0.6 + 0.1 * cos(x)$
Figs.(3 and 4) (f)	0.2	0.4	1	1	0.8	45	$0.6 + 0.1 * cos(x)$
Figs.(3 and 4) (h)	0.2	0.4	1	1	0.8	105	$0.6 + 0.1 * cos(x)$

Table 1: Parameter values used for numerical solution in both $1D$ and $2D$

4.2 Numerical solution in 2D

In this Subsection, we consider system (2.4) in a square domain and solve it on a grid of 100x100 sites, the spacing between the lattice points and the parameter values use here is defined as in $1D$. We plot only u, the spatial profiles of v are 180^0 out of phase with those of u. We present both the numerical and theoretical solutions side by side to see whether the two solutions conform to each other. The parameter values used for Figs. [4 are the same as in 3]. Similarly in $2D$, Figs. (4) are the same presentation as in Table 1.We compared the numerical solutions to those obtained by the linear stability theory and we observed that, the two solutions are in close agreement with each other.

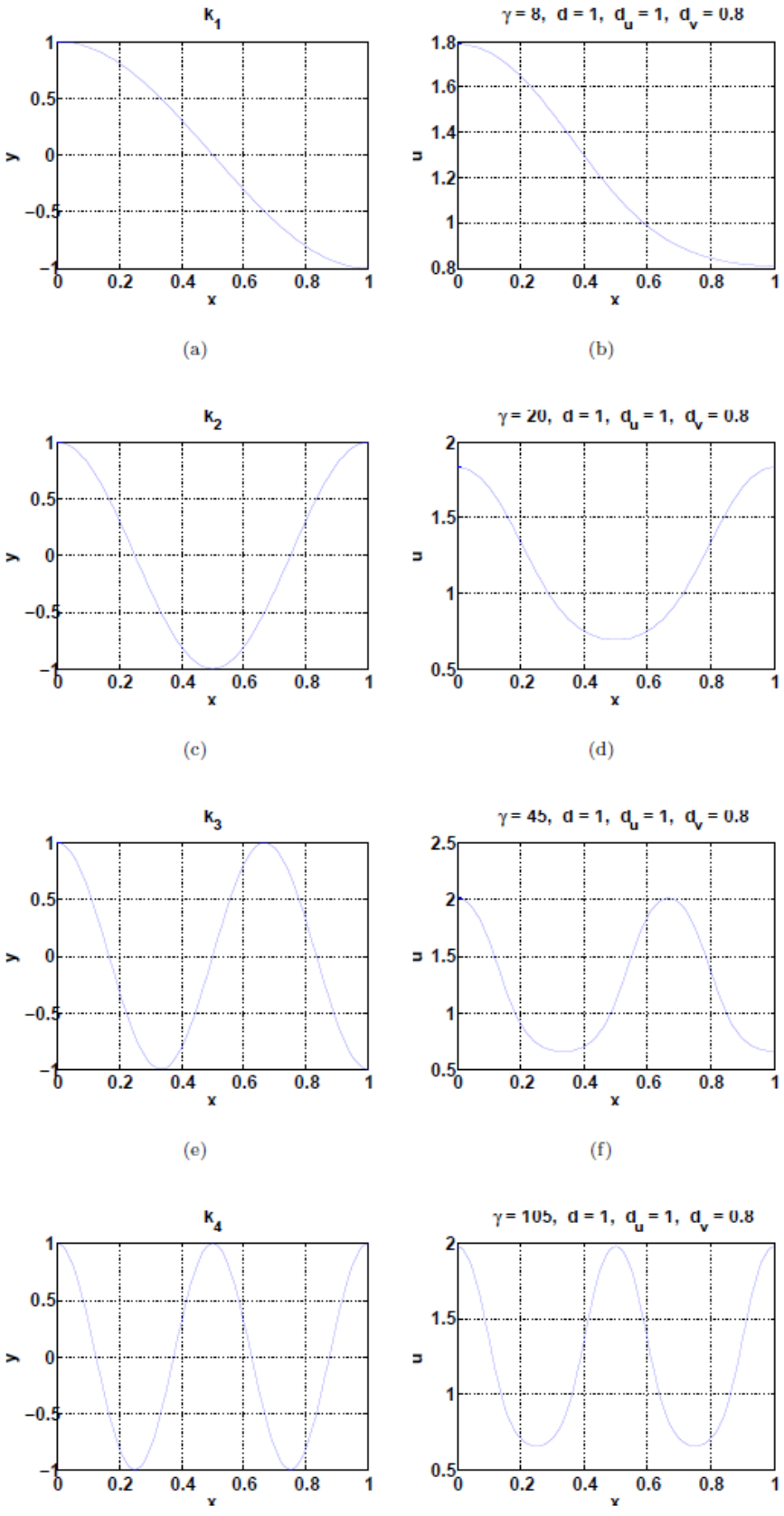

Figure 3: Linear stability solutions (left) with numerical solutions (right) in $\mathbf{1}\boldsymbol{D}$, with parameter values $a = 0.2, b = 0.4, d = 1, d_v = 0.8, d_u = 1$. [(b,d,f and h), $\gamma = 8, 20, 45$ and 105 respectively]. These shows that the numerical solutions (right) validate the theoretical results (left).

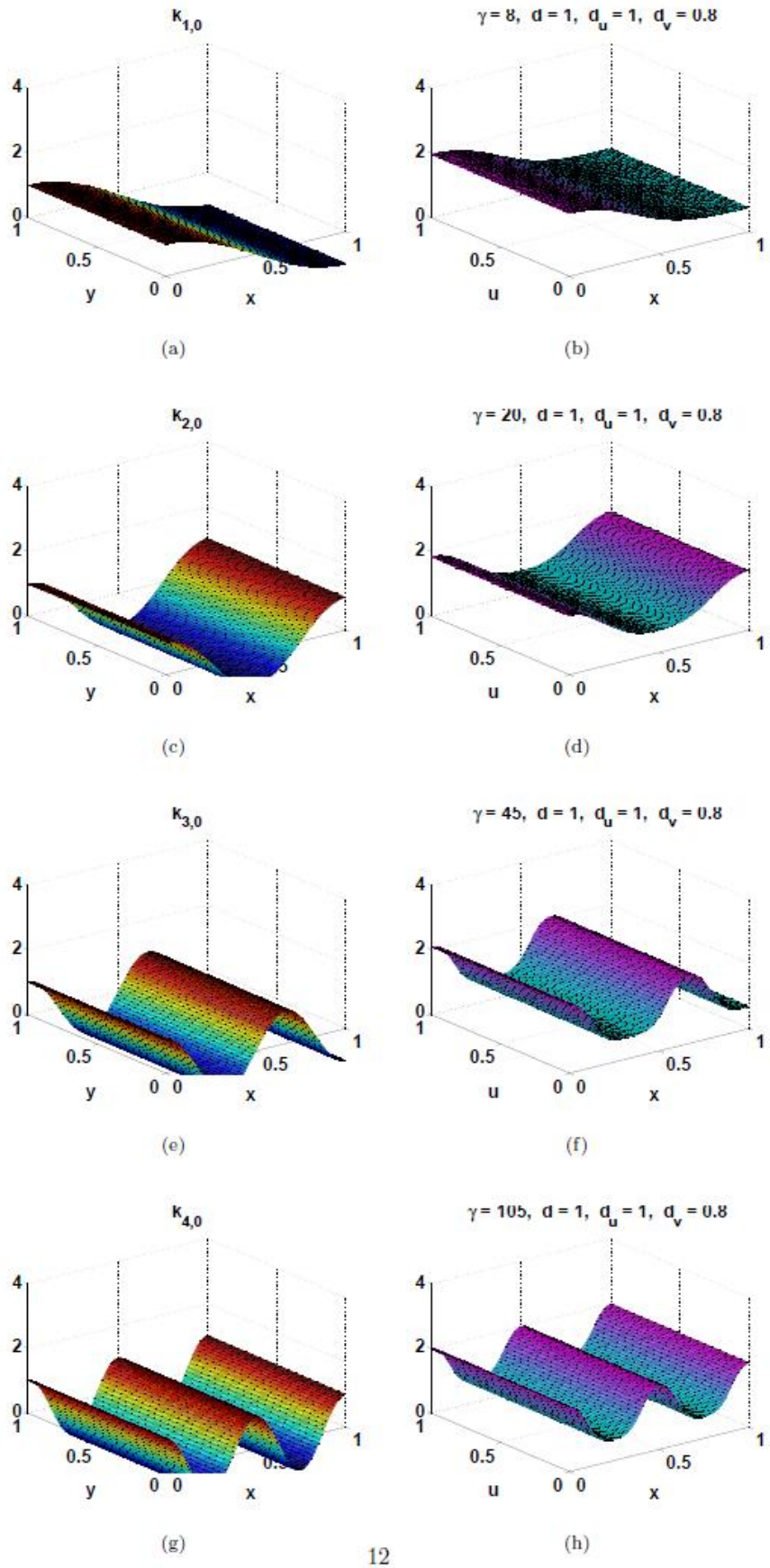

Figure 4: Linear stability solutions (left) with numerical solutions (right) in $\mathbf{2}\boldsymbol{D}$, with parameter values $a = 0.2, b = 0.4, d = 1, d_v = 0.8, d_u = 1$. [(b,d,f and h), $\gamma = 8, 20, 45$ and 105 respectively]. These shows that the numerical solutions (right) validate the theoretical results (left).

5 Conclusion

We have succeeded in deriving the necessary conditions for cross-diffusion-driven instability (also known as Turing cross-diffusion-driven instability) and the detailed linear stability analysis for reaction-diffusion systems with cross-diffusion were presented. We equally showed in details the finite difference method use in our numerical simulations, and to demonstrate the validity of our theoretical results, we solved numerically the model equations using finite difference method. We then use the numerical simulations to verify the theoretical results, and find that the numerical results are in close agreement to those predicted by the linear stability theory as we vary γ. Based on our results, we can conveniently state that, when the cross-diffusion coefficients are both absent that is $d_u = d_v = 0$ and the diffusion coefficient is unity ı.e $d = 1$, the emergence of spatial pattern is completely absent, see Fig. 2(d). But with the introduction of cross-diffusion coefficient, inspite the fact that the diffusion coefficient is unity ı.e. $d = 1$, there is an occurence of Turing space, see Figs.[2 (a), (b) and (c)].
The most important observation here is that, cross-difusion terms are necessary for the occurence of Turing instability and spatial pattern in the model. More precisely, with the help of the cross-diffusion coefficient along the u-component (d_v).

Finally, the solutions obtained shows that cross-diffusion plays an important role on the parameter spaces and spatial patterns.

Work is ongoing on the incorporation of domain growth, to see how the system will behave.

References

[1] Alimirantis Y. and Papageorgiou S. (1991). *Cross-diffusion effects on chemical and biological pattern formation.. J. Theor. Bio.* **151**: 289-311.

[2] Bard, J. and Lauder,I. (1974). "How well does Turing's Theory of morphogenesis work?" *J. Theor. Bio.* **45**:501-531.

[3] Barreira R., Elliott C.M., Madzvamuse A. (2011). The surface finite element method for pattern formation on evolving biological surfaces, *Journal of Math. Bio.* **63**, 1095-1119.

[4] Barrio R.A., Varea C., Aragon J.L., Maini P.K. (1999). A Two-dimensional Numerical study of Spatial Pattern Formation in Interacting Turing systems *Bulletin of Mathematical Biology*, **61**, 483-505.

[5] Bentil D.E and Murray J.D. (1993). On mechanical theory for biological pattern formation. *Physica D*, **63**:161-190.

[6] Chattopadhyay J. and Chatterjee S. (2001). *Cross-diffusional effect in a Lotka-Volterra competitive system. Nonlinear phenom complex syst*, **4**: 364-369.

[7] Chattopadhyay J. and Tapaswi P.K (1993). *Order and disorder in biological systems through negative cross-diffusion of mitotic inhibitor. Math. Comp. Model*, **17**: 105-112.

[8] Crampin E.J.Hackborn, W.W. and Maini,P.K. (2002). *Pattern formation in reaction-diffusion models with nonuniform domain growth. Bulletin of Mathematical Biology*,**64**:746-769.

[9] Epstein, I.R. and Pojman, J.A. (1998). *An introduction to nonlinear chemical dynamics (Topics in Physical Chemistry). Oxford University Press New York.*

[10] Federico R, Vanag K.V, Enzo T. and Epstein I. R. (2010). Quaternary cross diffusion in water-in oil microemulsions.

[11] Gambino, G. Lombardo, M.C. and Sammartino, M. (2012). Turing instability and traveling fronts for nonlinear reaction-diffusion system with cross-diffusion. *Maths. Comp. in Sim.* **82**:1112-1132.

[12] Gambino, G. Lombardo, M.C. and Sammartino, M. (2013). Pattern formation driven by cross-diffusion in 2-D domain. *Nonlinear Analysis: Real World Applications.* **14**:1755-1779.

[13] Gierer, A. and Meinhardt, H. (1972). A theory of biological pattern formation. *Kybernetik.* **12**:30-39.

[14] Gray,P. and Scott, S.K.(1990). *Chemical oscillations and instabilities. Nonlinear chemical kinetics. Oxford University Press, New York.*

[15] Gurtin M.E. (1974). *Some Mathematical models for population dynamics that lead segregation. Quart J. Appl. Math*, **32**: 1-8

[16] Hillen, T. and Painter, K.J.(2009). *A user's guide to PDE models for chemotaxis. J. Maths.Biol*,**58**:183-217.

[17] Iida, M. and Mimura, M. (2006). Diffusion, cross-diffusion an competitive interaction. J. Math. Biol. **53**:617-641.

[18] Kerner E.H(1959). *Further consideration on the statistical mechanics of biological associations. Bull. Math. Bio*, **21**: 217-255

[19] Kovács, S. (2004). Turing bifurcation in a system with cross-diffusion. *Nonlinear Analysis.* **59**:567-581.

[20] Li L., Jin Z and Sun G. (2008). Spatial pattern of an epidemic model with cross-diffusion. *Chin. Phys. Lett.* **25**:3500.

[21] Madzvamuse A. (2000). A Numerical approach to the study of spatial pattern formation *D.Phil Thesis*, University of Oxford.

[22] Madzvamuse A., Gaffney, E.A. and Maini,P.K.(2010). *Stability Analysis of non-autonomous reaction-diffusion systems: the effects of growing domains.J.Maths. Biol.* **61**(1):133-164

[23] Madzvamuse A; Maini, P.K. and Wathen,A.J.(2003) *A moving grid finite element method applied to a model biological pattern generator.J.Comp. Phys.* **190**:478-500.

[24] Madzvamuse A, Roger K. Thomas., Philip K. Maini., Andrew J. Wathen. (2002). A Numerical Approach to the Study of Spatial Pattern Formation in the Ligaments of Arcoid Bivalves. *Bulletin of Mathematical Biology.* **64**:501-530.

[25] Madzvamuse A, Ndakwo H.S. and Barreira R. (2014). Cross-diffusion-driven instability for reaction-diffusion systems: Analysis and simulations. *J. Maths. Biol. submitted.*

[26] Marten S., Steve C., Jonathan A. F., Carl F. and Brain W. (2001). *Catastrophic shifts in ecosystems, Nature.* **413**:591-596.

[27] Max R., Stefan C. D., Peter. C. De R, and Johan V. De K. (2004). *Self-organized patchiness and Catastrophic shifts in ecosystems, Science.* **305**:1926-1929.

[28] McAfree, M.S. and Annunziata, O. (2013). Cross-diffusion in a colloidpolymer aqueous system. *Fluid Phase Equilibria.* **356**:46-55.

[29] McDougall T. and Turner J.S. (1982). *Influence of cross-diffusion on finger double-diffusive convection. Nature.* **299**:812-814.

[30] Morton K.W. and Mayers D.F. (1994). Numerical Solution of Partial Differential Equations. Cambridge University Press.

[31] Murray J.D. (1982). Parameter space for Turing instability in reaction diffusion mechanisms: A comparison of models. *J. Theor. Bio.* **98**:143-163.

[32] Murray J.D. (2003). Mathematical Biology II: Spatial models and biomedical applications. Third Edition. Springer.

[33] Prigogine, I. and Lefever, R. (1968). Symmetry breaking instabilities in dissipative systems. II. *J. Chem. Phys.* **48**, 1695-1700.

[34] Ruiz-Baier, R. and Tian, C. (2013). Mathematical analysis and numerical simulation of pattern formation under cross-diffusion. *Nonlinear Analysis: Real World Applications.* **14**: 601-612.

[35] Schnakenberg, J. (1979). Simple chemical reaction systems with limit cycle behaviour. *J. Theor. Biol.*, **81**:389-400.

[36] Tian, Lin, Z. and Pedersen, M. (2010). Instability induced by cross-diffusion in reaction-diffusion systems. *Nonlinear Analysis: Real World Applications.* **11**:1036-1045.

[37] Turing, A. (1952). On the chemical basis of morphogenesis. *Phil. Trans. Royal Soc. B.* **237**: 37-72

[38] Uduak, Z.G. (2011). A Numerical approach to the studying cell dynamics. *D.Phil Thesis*, University of Sussex.

[39] Vanag, V.K. and Epstein, I.R. (2009). Cross-diffusion and pattern formation in reaction diffusion systems. *Physical Chemistry Chemical Physics.* **11**:897-912.

[40] Xie, Z. (2012). Cross-diffusion induced Turing instability for a three species food chain model. *J. Math. Analy. and Appl.* **388**: 539-547.

[41] Yi W., Jianzhong W. and Li Z. (2010). *Cross-diffusion-induced pattern in an SI model Appl. Math. and Com.* **217**: 1965-1970.

[42] Zhabotinsky, A.M. (1991.) *A history of chemical oscillations and waves.Chaos.* **1**:379-386.

[43] Zhang, J.F, Li, W.T, Wang, Y.X.(2011). *Turing patterns of a strongly coupled predator prey system with diffusion effects.Nonlinear Analysis.* **74**:847-858.

[44] Zemskov, E.P., Vanag, V.K. and Epstein, I.R. (2011). Amplitude equations for reaction-diffusion systems with cross-diffusion. *Phys. Rev. E.* **84**:036216.